

Diastolic Function In Normal Sinus Rhythm Vs. Chronic Atrial Fibrillation: Comparison By Fractionation Of E-Wave Deceleration Time Into Stiffness And Relaxation Components

Sina Mossahebi, Sándor J. Kovács

Cardiovascular Biophysics Laboratory, Cardiovascular Division, Department of Medicine, Washington University School of Medicine, St. Louis, MO, USA.

Abstract

Although the electrophysiologic derangement responsible for atrial fibrillation (AF) has been elucidated, how AF remodels the ventricular chamber and affects diastolic function (DF) has not been fully characterized. The previously validated Parametrized Diastolic Filling (PDF) formalism models suction-initiated filling kinematically and generates error-minimized fits to E-wave contours using unique load (x_0), relaxation (c), and stiffness (k) parameters. It predicts that E-wave deceleration time (DT) is a function of both stiffness and relaxation. Ascribing DT_s to stiffness and DT_r to relaxation such that $DT = DT_s + DT_r$ is legitimate because of causality and their predicted and observed high correlation ($r=0.82$ and $r=0.94$) with simultaneous (diastatic) chamber stiffness (dP/dV) and isovolumic relaxation (tau), respectively.

We analyzed simultaneous echocardiography-cardiac catheterization data and compared 16 age matched, chronic AF subjects to 16, normal sinus rhythm (NSR) subjects (650 beats). All subjects had diastatic intervals. Conventional DF parameters (DT , AT , E_{peak} , E_{dur} , $E-VTI$, E/E') and E-wave derived PDF parameters (c, k, DT_s , DT_r) were compared. Total DT and DT_s , DT_r in AF were shorter than in NSR ($p<0.005$), chamber stiffness, (k) in AF was higher than in NSR ($p<0.001$). For NSR, 75% of DT was due to stiffness and 25% was due to relaxation whereas for AF 81% of DT was due to stiffness and 19% was due to relaxation ($p<0.005$).

We conclude that compared to NSR, increased chamber stiffness is one measurable consequence of chamber remodeling in chronic, rate controlled AF. A larger fraction of E-wave DT in AF is due to stiffness compared to NSR. By trending individual subjects, this method can elucidate and characterize the beneficial or adverse long-term effects on chamber remodeling due to alternative therapies in terms of chamber stiffness and relaxation.

Introduction

Atrial fibrillation (AF) is a known correlate of heart failure (HF) and affects millions of patients worldwide. Investigators have demonstrated that AF and HF are concordant and increase overall mortality rate.¹⁻⁴ Significant progress has been made in the diagnosis, electrophysiologic mechanism, and treatment of AF.¹⁻¹⁰ However, the mechanistic consequences of AF on left ventricular (LV) function, chamber stiffness and relaxation, and global LV diastolic function (DF) in particular, remain incompletely characterized.

Key Words:

LV Stiffness, LV Relaxation, Diastolic Function, Atrial Fibrillation, E-Wave DT.

Disclosures:
None.

Corresponding Author:
Sándor J. Kovács, PhD, MD
Cardiovascular Biophysics Laboratory
Washington University Medical Center
660 South Euclid Ave, Box 8086.
St. Louis, MO. 63110

The instantaneous slope of the left ventricular (LV) pressure-volume relation, dP/dV, defines chamber stiffness and serves as one of the two main parameters (the other is relaxation) by which global diastolic function (DF) is quantitated.¹¹⁻¹⁴ Traditionally, LV chamber stiffness is determined invasively from the slope ($\Delta P/\Delta V$) of the end-diastolic pressure volume relationship (EDPVR). However, due to the lack of atrial contraction, end-diastole in AF and NSR are different physiologic states. Hence the EDPVR cannot be used to compare the chamber stiffness in AF with that in NSR. Therefore, the diastatic pressure volume relationship (D-PVR) provides the appropriate physiologic metric for AF vs. NSR chamber stiffness comparison. It has been established that (passive) diastatic chamber stiffness, i.e. the slope of D-PVR, is significantly elevated in AF compared to NSR.¹⁵

Chamber stiffness ($\Delta P/\Delta V$) is a 'relative' index and can be determined using 'relative' (echo), rather than 'absolute' (cath) measurement methods. Little et al¹⁶ used physiologic modeling to predict that E-wave DT is determined by stiffness (K_{LV}) alone. However, for E-wave contours well fit by underdamped oscillatory kinematics, the PDF formalism¹⁷ parameter k is the algebraic

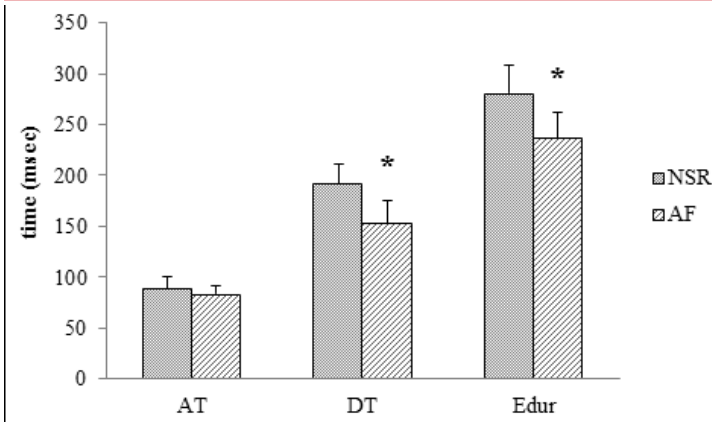


Figure 1: AT, DT, and Edur determined by approximating E-wave shape as a triangle in NSR group (16 subjects) and AF group (16 subjects). Significant differences between DT and Edur are denoted by asterisk (*). (DT: $p < 0.001$, Edur: $p < 0.001$) between groups. See Table 2 and text for details.

equivalent of K_{LV}

Clinicians know that tall, narrow E-waves having a short DT, referred to as the ‘constrictive-restrictive’ pattern, are associated with stiff chambers. Similarly, long DT is referred to as a manifestation of the ‘delayed relaxation’ pattern. Therefore, from an intuitive clinical perspective it is self-evident that both stiffness and relaxation must be DT determinants. This intuitive role of stiffness and relaxation as DT determinants has been made physiologically precise by Shmuylovich et al who have shown that two subjects having echocardiographically indistinguishable DT can have significantly distinguishable values of chamber stiffness and relaxation (τ) on simultaneous hemodynamic analysis. Using PDF-based analysis, the derived algebraic expression for DT was shown to be a function of both stiffness (PDF parameter k) and relaxation (PDF parameter c).¹⁸ The aforementioned naturally justifies decomposition of E-wave DT into its stiffness (DT_s) and relaxation (DT_r) components such that $DT = DT_s + DT_r$.¹⁹ The expected causal relationship between DT_s and DT_r and simultaneous stiffness ($\Delta P/\Delta V$) and relaxation (τ) has been firmly established by the high observed correlation ($r=0.82$ and $r=0.94$ respectively).¹⁹

We hypothesized that AF LVs are stiffer than NSR LVs. Consequently, decomposition of E-wave DT into stiffness (DT_s) and relaxation (DT_r) components will show that, compared to NSR, DT_s is shorter in AF and a larger percentage of E-wave DT in AF is due to stiffness than to relaxation.

Material And Methods

Subject Selection

Thirty two datasets (mean age 61, 22 men) were selected from the Cardiovascular Biophysics Laboratory database.²⁰ Subjects underwent elective cardiac catheterization to determine presence of suspected coronary artery disease at the request of their referring physicians. All participants provided informed consent prior to the procedure using a protocol approved by the Washington University Human Research Protection Office (HRPO).

Sixteen datasets of subjects in NSR, were selected so they were aged matched with the 16 subjects of the chronic AF group (average duration 7.3 ± 4.1 years). All were in AF during data acquisition. Selection criteria for the NSR group were: no active ischemia, normal valvular function, normal LV ejection fraction ($LVEF \geq 50\%$), no history of myocardial infarction, peripheral vascular disease, or bundle branch block, and clear diastatic intervals following E-waves.

Selection criteria for the AF group were similar, with the exception that four of the 16 AF subjects had LVEF somewhat $< 50\%$. Among the 16 NSR datasets, 9 had normal LV end-diastolic pressure ($LVEDP < 14$ mmHg), 3 had 15 mmHg $< LVEDP < 20$ mmHg and 4 had elevated LVEDP (> 21 mmHg). The distribution of LVEDPs in the 15 AF group datasets were: 3 with $LVEDP < 14$, 9 with $15 < LVEDP < 20$ mmHg and 4 with $LVEDP > 21$. A total of 650 cardiac cycles (20 beats/subject) of simultaneous echocardiographic-high fidelity hemodynamic (conductance catheter) data were analyzed. The clinical descriptors of the 32 subjects and their hemodynamic and echocardiographic indices are shown in Table 1 and 2.

Data Acquisition

The high fidelity, simultaneous echocardiographic transmitral flow and pressure-volume (P-V) data recording method has been previously described [17,20-24]. Briefly, immediately prior to arterial access a complete 2-D echo-Doppler study in a supine position using a Philips (Andover, MA.) iE33 system is performed according to American Society of Echocardiography (ASE) criteria.²⁵ After arterial access and placement of a 64-cm, 6-Fr sheath (Arrow, Reading, PA), a 6-Fr micromanometer conductance catheter (SPC-560, SPC-562, or SSD-1034, Millar Instruments, Houston, TX) was directed across the aortic valve under fluoroscopic control. Pressure and volume signals were processed through clinical amplifier systems (Quinton Diagnostics, General Electric, CD Leycom) and recorded by a custom personal computer via a standard interface (Sigma-5). Simultaneous transmitral Doppler images were obtained [25] using a clinical imaging system (Philips iE33, Andover, MA). Following data acquisition, end-systolic and end-diastolic volumes (ESV, EDV) were determined by calibrated quantitative ventriculography.

Doppler E-Wave Analysis

For each subject, approximately 1-2 minutes of continuous transmitral flow data were recorded in the pulsed-wave Doppler mode. Echocardiographic data acquisition is performed in accordance with published ASE²⁶ guidelines. In accordance with convention, the apical 4-chamber view was used for Doppler E-wave recording with the sample volume located at the leaflet tips. An average of 20 beats per subject were analyzed (650 cardiac cycles total for the 32 subjects).

Doppler transmitral E-wave contours were analyzed using the conventional triangle shape approximation,^{27,28} yielding peak E-wave velocity (E_{peak}), acceleration time (AT), deceleration time (DT),

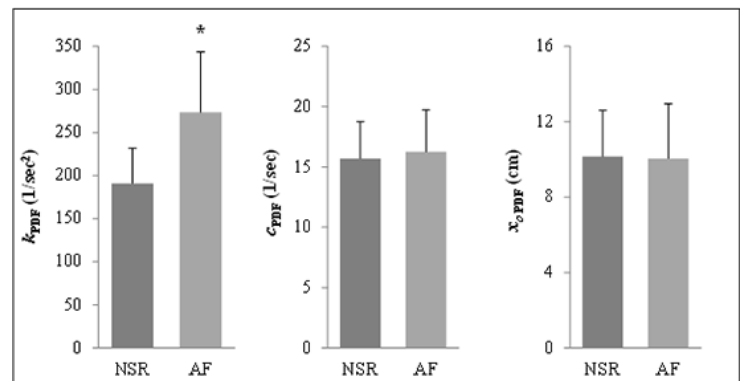


Figure 2: PDF parameters (k , c , and x_0) in NSR group (16 subjects) and AF group (16 subjects). Significant ($p < 0.001$) differences between groups for k are denoted by asterisk (*) indicating that AF chambers at diastasis are stiffer than NSR chambers at diastasis. See text

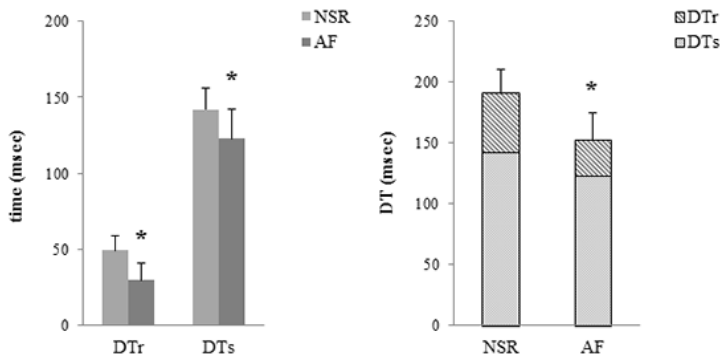


Figure 3: A) Comparison of stiffness (DT_s), relaxation (DT_t) components of total DT according to group. Asterisk (*) indicates DT_s and DT_t are both significantly shorter in AF than in NSR. B) Comparison of total DT between groups indicates significant difference (*). When DT is decomposed into its DT_s , DT_t components in NSR and AF groups, significant intergroup differences in components persist as shown in Panel A. See text for details.

velocity-time integral (E-VTI), E/E'.

Each E-wave was also analyzed via the Parametrized Diastolic Filling (PDF) formalism (see Appendix 1) to yield, mathematically unique PDF parameters for each E-wave (stiffness parameter (k), chamber viscoelasticity/relaxation parameter (c), load parameter (x_0)).^{23,29,30}

Stiffness (DT_s) and relaxation (DT_t) components of DT were computed via the fractionation method employed previously¹⁹ (see Appendix 2) such that $DT = DT_s + DT_t$. By determining DT_s and DT_t of each E-wave, the total DT can be expressed as the fraction due to stiffness ($S = DT_s / DT$) and the fraction of DT due to relaxation ($R = DT_t / DT$) for each E-wave analyzed.

Determination Of Diastatic Stiffness From P-V Data

Hemodynamics were determined from the high-fidelity Millar LV P-V data from each beat. The quantitative ventriculography was used to determine end-systolic and end-diastolic volumes which defined the limits of volume tracing of conductance catheter has been previously detailed.^{23,24,31,32} After calibration of conductance volume, LV pressure and volume at diastasis were measured beat-by-beat using a custom MATLAB program. End-diastasis points were defined by ECG P wave onset.^{24,31-33} As previously^{24,32} for each subject, diastatic P-V data points generated by load varying cardiac cycles were fit via linear regression, to provide diastatic chamber stiffness as the slope (K) of D-PVR.

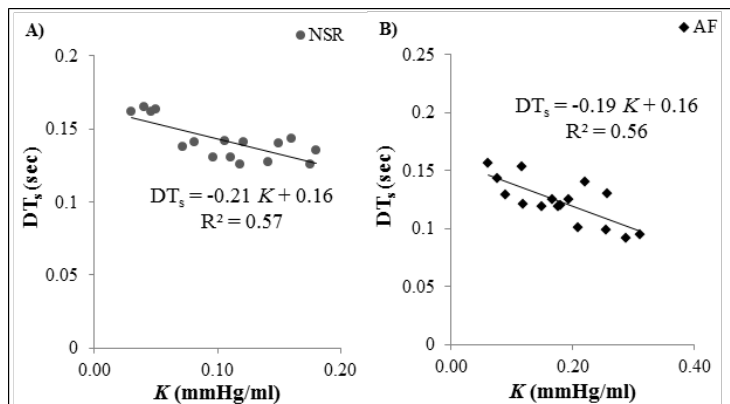


Figure 4: A) Least mean square determined linear fit of stiffness component of DT (DT_s) vs. diastatic stiffness (K) in A) 16 NSR subjects, B) 16 AF subjects. See text for details.

Medications

The classes of prescribed medications among the 16 subjects of the AF group were as follows: 14 on anticoagulants/antithrombotics, 9 on beta blockers, 7 on lipid lowering agents, 7 on ACE inhibitor or ARB, 6 on calcium channel blockers, 6 on diuretics, and 5 on digoxin.

Statistical Analysis

For each subject, parameters were averaged for the beats selected. Comparisons of diastatic stiffness, AT, DT, E_{dur} , PDF parameters, and other parameters between NSR and AF groups were carried out by Student's t-test using MS-Excel (Microsoft, Redmond, WA).

Results

Diastatic Stiffness And Other Invasive Measurements In NSR And AF

LV (passive) chamber stiffness measured as the slope of the D-PVR is significantly higher in the AF group than that in the NSR group (0.18 ± 0.08 mmHg/ml vs. 0.11 ± 0.05 mmHg/ml, $p < 0.01$). In contrast to NSR, (where diastatic pressure and volume is different than end-diastolic pressure and volume at end atrial systole), in AF, diastatic pressure and volume is the same as end-diastolic pressure and volume since there is no atrial contraction in AF. In AF diastatic pressure and volume are similar to the diastatic pressure and volume in NSR (18 ± 4 mmHg for AF vs. 17 ± 5 mmHg for NSR, $p = 0.48$ and 167 ± 55 ml for AF vs. 159 ± 12 ml for NSR, $p = 0.59$).

Triangle Method Measurements Of E-waves In NSR And AF

Figure 1 shows that E-wave DT and E-wave duration (E_{dur}) are significantly shorter in the AF group than NSR group (DT: 153 ± 22 msec vs. 192 ± 19 msec, $p < 0.001$, E_{dur} : 236 ± 26 msec vs. 281 ± 27 msec, $p < 0.001$). E-wave acceleration time (AT) is not significantly different between the two groups (84 ± 8 msec vs. 89 ± 11 msec, $p = 0.13$).

PDF Measurements In NSR And AF

Results from PDF analysis show (Figure 2) that PDF stiffness parameter (k) in AF group is higher (stiffer) than NSR group (274 ± 70 1/sec² vs. 191 ± 41 1/sec², $p < 0.001$). PDF parameters c, x_0 are not significantly different between AF and NSR groups (c: 15.7 ± 3.0 1/sec vs. 16.3 ± 3.5 1/sec, $p = 0.65$ and x_0 : 10.2 ± 2.5 cm vs. 10.1 ± 2.9 cm, $p = 0.93$).

Fractionation Of Deceleration Time Into Stiffness And Relaxation Components In NSR And AF

Figure 3 shows the stiffness and relaxation components in both groups and their contribution to DT. The relaxation (DT_t) component

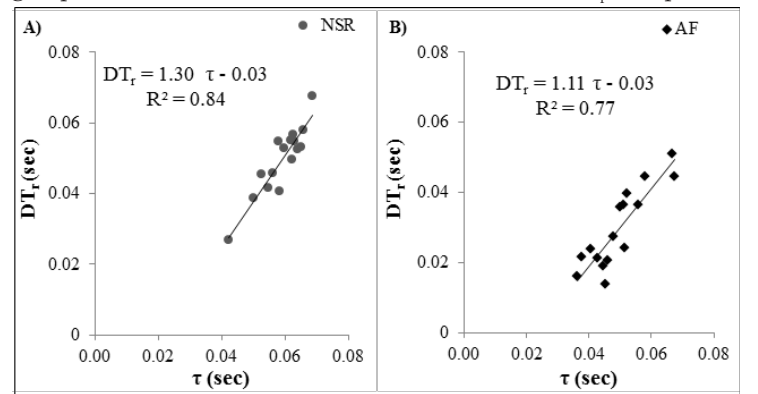


Figure 5: A) Least mean square determined linear fit of relaxation component of DT (DT_t) vs. time constant of isovolumic relaxation (τ) in A) 16 NSR subjects, B) 16 AF subjects. See text for details.

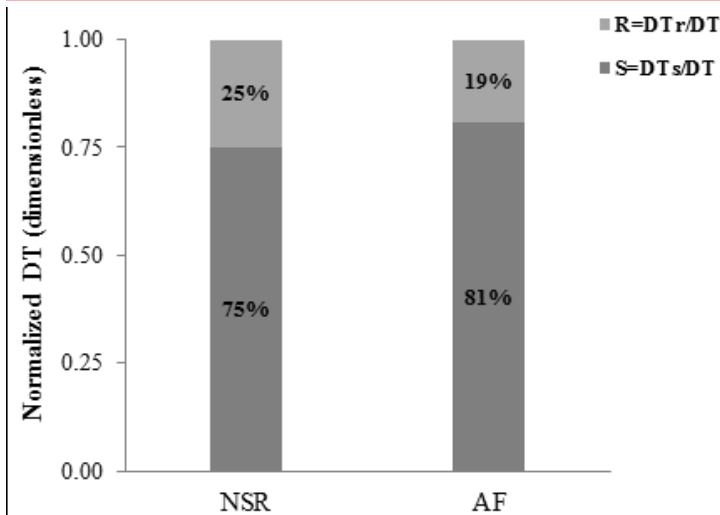


Figure 6: Intergroup comparison of normalized DT showing percentage due to stiffness (S) and relaxation (R). A significantly larger percentage of total DT is due stiffness in the AF group. See text for details.

of DT in AF is shorter than in NSR (DT_r AF=30±12 vs. DT_r NSR=50±10, $p<0.001$). The stiffness (DT_s) component of DT in AF, which is inversely related to chamber stiffness, is shorter than in NSR (DT_s AF=123±20 vs. DT_s NSR=142±14, $p<0.005$). The shorter DT_s in AF and the known inverse relation between DT_s and (diastatic) stiffness indicates that AF chambers are stiffer than NSR chambers. DT_s and diastatic stiffness derived from P-V data (K) were highly correlated in both NSR and AF groups (NSR: $DT_s = -0.21 K + 0.16$, $R^2=0.57$, AF: $DT_s = -0.19 K + 0.16$, $R^2=0.56$) (Figure 4). DT_r and time constant of isovolumic relaxation (τ) were highly correlated in both NSR and AF groups (NSR: $DT_r = 1.30 \tau - 0.03$, $R^2=0.84$, AF: $DT_r = 1.11 \tau - 0.03$, $R^2=0.77$) (Figure 5).

For the 16 NSR datasets 75% of total DT is due to stiffness and 25% is due to relaxation. For the 16 AF datasets 81% of DT is due to stiffness and 19% is due to relaxation (Figure 6). These differences are significant ($p<0.005$). If the four AF subjects with LVEF <50% are removed from the intergroup comparison, all of the conclusions remain unaltered.

Discussion

Invasive And Non-Invasive Measurements Of AF Chamber Stiffness

Although multiple methods for LV chamber stiffness determination using echocardiography have been proposed,^{16,23,34,35} one of the most important methods for characterizing passive chamber stiffness has been the end-diastolic pressure volume relation (EDPVR), defined by the locus of points inscribed by end-diastolic pressures and volumes at varying loads.¹¹ Considering the EDPVR in the setting of chronic AF raises a concern, however. Because there is no atrial contraction, end-diastole in (rate controlled) AF is the hemodynamic equivalent of diastasis. During diastasis the ventricle is in static equilibrium (for a brief period), atrial and ventricular pressures are equal and net transmitral flow is absent.³⁶ This equivalence between end-diastole and diastasis does not exist in NSR, and previous work [32] has shown that in the same NSR heart, the D-PVR and EDPVR are physiologically distinct relations, with significantly different slopes and therefore different values for chamber stiffness. Hence, the D-PVR is the only physiologically justified invasive method available for chamber stiffness determination in AF. The use of D-PVR requires the determination of load-varying diastatic pressure and volume points.

In addition to invasive approaches, the stiffness of the LV chamber can also be estimated noninvasively. The PDF parameter k obtained from echocardiographic E-wave analysis is mathematically¹⁷ and experimentally related to the invasively measured chamber stiffness ($\Delta P/\Delta V$) during early rapid filling²³ E-wave deceleration time (DT) has also been correlated with stiffness as proposed by Little et al.¹⁶ It was shown that an inverse square relationship exists between stiffness and E-wave DT.

Both the triangle based (DT) and PDF model based (k) non-invasive estimates of chamber stiffness showed significant difference between the AF and NSR groups, consistent with the invasive chamber stiffness findings between groups at diastasis.¹⁵ The significantly shorter DT in the AF group is not likely to be explained by the higher average HR of the AF group since it is known that in the presence of a diastatic interval, E-wave DT remains essentially unchanged when HR increases.³⁷

Deceleration Time Of E-wave Correlation With Chamber Stiffness And Relaxation

Average left ventricular (LV) chamber stiffness, $\Delta P/\Delta V$, is an important diastolic function (DF) metric. An E-wave based determination of $\Delta P/\Delta V$ by Little et al predicted that deceleration time (DT) is related to stiffness according to $\Delta P/\Delta V = A/(DT)^2$.¹⁶ This implies that if the DTs of two LVs are indistinguishable, their stiffness should be similarly indistinguishable. Shmuylovich et al.¹⁸ have shown that two subjects with indistinguishable E-wave determined DTs can have distinguishable catheterization-determined values of chamber stiffness, because of differences in relaxation, i.e. the viscoelastic parameter (PDF parameter c) in the two subjects. We found E-wave DT and its stiffness component are significantly (DT : $p<0.001$, DT_s : 0.005) shorter in the AF group ($DT=153\pm 22$ msec, $DT_s=123\pm 20$) than NSR group ($DT=192\pm 19$ msec, $DT_s=142\pm 14$). The shorter DT in AF group is primarily an effect of stiffness because the relaxation parameter c is similar in the two groups ($p=0.65$).

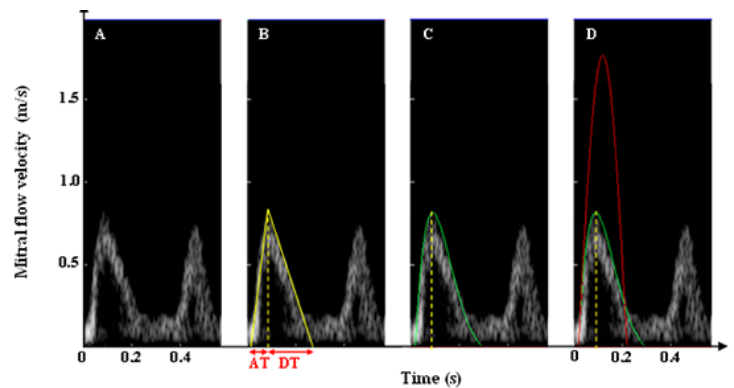


Figure 7: Overview of DTs and DT_r computation. A) A typical Doppler velocity profile. Note diastatic interval between E- and A-waves. B) AT and DT determination using triangle method. C) PDF model-predicted fit to E-wave (green) provides numerically unique PDF parameters $c=21.8/s$, $k=248/s^2$, $x_0=11.2cm$ for each analyzed E-wave. D) Model predicted E-wave (red) having same x_0 , k values as original (green) E-wave but with PDF parameter $c=0$, assumes relaxation plays no role in determining waveform. The effect of relaxation (where $c\neq 0$) is to lengthen DT and decrease E-wave amplitude. Hence, green DT is longer and its amplitude is less than red waveform. The numerical difference between actual green ($c\neq 0$) DT minus red DT ($c=0$) equals DT_r . $DT_s = DT - DT_r$. $DT=0.206$ s, $DT_r=0.077$ s and $DT_s=0.129$ s. See text for details.

Table 1: The clinical descriptors of NSR and AF groups.

Clinical Descriptors	NSR Group	AF Group	Significance
N	16	16	N.A.
Age (y)	61±8	61±9	0.92
Gender (M/F)	10/6	12/4	N.A.
Heart Rate (bpm)	62±9	76±9	<0.001
Ejection Fraction (LVEF) (%)	73±8	55±17	<0.01
Height (cm)	172±10	178±10	N.S.
Weight (kg)	89±14	99±18	N.S.
CHA2DS2-VASc factors			
Female gender	6	4	N.A.
Heart failure	0	4	N.A.
Hypertension	7	13	N.A.
Age 65 to < 74 years	4	5	N.A.
Age > 75	2	1	N.A.
Diabetes mellitus	0	0	N.A.
Stroke	0	0	N.A.
Vascular disease	0	0	N.A.

Data are presented as mean ± standard deviation.

LVEF left ventricular ejection fraction (via calibrated ventriculography)

NSR normal sinus rhythm.

AF atrial fibrillation.

N.S. not significant

N.A. not applicable

Decomposition Of E-wave Deceleration Time To Stiffness And Relaxation Components

Because E-wave DT depends on both stiffness (k) and relaxation (c) we have previously proposed¹⁹ a method by which E-wave DT can be decomposed to stiffness (DT_s) and relaxation (DT_r) components. We have shown¹⁹ that DT_s was highly correlated ($r=0.82$) with (simultaneous) invasively determined (passive) diastatic chamber stiffness, and DT_r and the time-constant of IVR (τ) from simultaneous high fidelity pressure data and IVRT determined by echocardiography were highly correlated ($r=0.94$, $r=0.89$).

In the current study we analyzed simultaneous LV P-V and transmitral flow (echo) data and decomposed E-wave DT in to stiffness (DT_s) and relaxation (DT_r) components in NSR and AF groups. As expected diastatic stiffness and PDF stiffness parameter k were higher in AF group compared to NSR group and AF E-wave DT was shorter than in NSR. Figure 6 shows the fraction of DT accounted for by stiffness (S) in the AF group is significantly higher than in the NSR group ($p<0.005$), and the fraction of DT due to the relaxation (R) in the AF group is significantly lower than in the NSR group ($p<0.005$). Although the numerical value of the PDF relaxation parameter c is similar in NSR and AF, the fraction of the total DT due to relaxation ($R = DT_r / DT$ (%)) is less in AF than in NSR because DT and DT_r in AF group is shorter (See Fig. 3) than in NSR. This is underscored by the difference in stiffness parameter k , being higher (stiffer) in AF vs NSR. This method is totally general. It fractionates total DT into its stiffness and relaxation components and thereby reflects actual chamber properties. As such, the method allows for longitudinal assessment and trending of beneficial vs. adverse effects of alternative treatment strategies on chamber properties of stiffness and relaxation in clinical settings where echocardiography is utilized.

Limitations

Conductance Volume

The conductance catheter method of volume determination has

Table 2: Hemodynamic and echocardiographic data in NSR and AF groups

	NSR	AF	Significance
Hemodynamic Parameters:			
LVEDP (mmHg)	17±5	18±4	0.48
Gender (M/F)	10/6	12/4	N.A.
LVEDV (ml)	159±12	167±55	0.59
Diastatic stiffness (mmHg/ml)	0.11±0.05	0.18±0.08	<0.01
τ (msec)	59±7	50±10	<0.01
Echocardiographic Parameters			
Peak E-wave velocity (Epeak) (cm/s)	71±15	89±26	<0.05
E-wave acceleration time (AT) (ms)	89±11	84±8	0.13
E-wave deceleration time (DT) (ms)	192±19	153±22	<0.001
E-wave duration time (Edur) (ms)	281±27	236±26	<0.001
E/E' (dimensionless)	4.7±1.8	6.0±1.9	<0.05
x_0 (cm)	10.2±2.5	10.1±2.9	0.93
k (1/sec ²)	191±41	274±70	<0.001
c (1/sec)	15.7±3.0	16.3±3.5	0.65
DT_r (msec)	50±10	30±12	<0.001
DT_s (msec)	142±14	123±20	<0.005
$R = DT_r / DT$ (%)	25±3	19±7	<0.005
$S = DT_s / DT$ (%)	75±3	81±7	<0.005

Data are presented as mean ± standard deviation.

LVEDP left ventricular end-diastolic pressure

LVEDV left ventricular end-diastolic volume

τ time constant of isovolumic relaxation

E/E' ratio of Epeak and E'peak

E-VTI E-wave velocity-time integral

k PDF stiffness parameter

c PDF relaxation parameter

DT_r relaxation component of DT

DT_s stiffness component of DT

known limitations related to noise, saturation and calibration that we have previously acknowledged.^{17,20-24,32} In this study, the channels which provided physiologically consistent P-V loops were selected and averaged. However, since there was no significant volume signal drift during recording, any systematic offset related to calibration of the volume channels did not affect the result when the limits of conductance volume were calibrated via quantitative ventriculography.

HR Limitation

The D-PVR is defined by a linear, least mean-squared error fit to the load varying locus of points at which diastasis is achieved. At elevated heart rates diastasis is usually eliminated. In this study datasets were selected such that for every analyzed cardiac cycle in AF or NSR a clear, diastatic interval was present after E-wave termination, prior to the onset of the next systole in AF, or prior to the onset of the Doppler A-wave in NSR.

Sample Size

Although the number of subjects ($n=32$) is modest, and may be viewed as a minor limitation regarding statistics, the total number of cardiac cycles analyzed ($n=650$) mitigates the sample size limitation to an acceptable degree.

Conclusions

We used the PDF formalism to decompose E-wave deceleration time into its stiffness and relaxation components in NSR and AF groups where E-waves were always followed by a diastatic interval. We found that AF chambers have increased (diastatic) stiffness compared to NSR chambers at diastasis. In addition, a larger percentage of

E-wave DT in AF is due to stiffness than to relaxation compared to NSR. This novel method allows clinicians to track and trend the effect of alternative pharmacologic therapies in terms of DT_s and DT_r , not only as DF determinants, but as metrics of beneficial vs. adverse remodeling and as determinants of prognosis and rehospitalization in clinical settings where echocardiography is employed.

Acknowledgments

This work was supported in part by the Alan A. and Edith L Wolff Charitable Trust, St. Louis, and the Barnes-Jewish Hospital Foundation. Sina Mossahebi was supported in part by a teaching assistantship from the Physics Department, Washington University College of Arts and Sciences. We thank sonographer Peggy Brown for expert echocardiographic data acquisition, and the staff of Barnes Jewish Hospital Cardiovascular Procedure Center's Cardiac Catheterization Laboratory for their assistance.

Appendix 1

The PDF Formalism

The kinematics of filling is modeled using the Parameterized Diastolic Filling (PDF) formalism which uses a linear, bi-directional spring to approximate early filling in accordance with the velocity of a damped SHO.²⁹ In accordance with Newton's second law, the equation of motion is:

$$\frac{d^2x}{dt^2} + c \frac{dx}{dt} + kx = 0 \quad [A.1]$$

Because the E-wave has zero initial velocity, the model's initial velocity is zero ($v(0)=0$). However, the SHO has a non-zero initial spring displacement, x_0 . Systole stores elastic strain in tissue, which at mitral valve opening, is available to power mechanical recoil and the ventricular suction process. Equation 1 allows calculation of parameters c and k per unit mass. The predicted contour of the clinical E-wave is obtained from the solution for the SHO velocity. The underdamped solution is:

$$v(t) = -\frac{x_0 k}{\omega} \exp(-ct/2) \sin(\omega t) \quad [A.2]$$

where . The determination of PDF parameters from each E-wave solves the 'inverse problem' of diastole and generates a unique set of x_0 , c , and k ³⁸ values for each contour. The three parameters x_0 , c , and k encompass the (lumped) physiologic determinants of all E-wave contours. The initial oscillator displacement x_0 (cm) is linearly related to the velocity-time integral (VTI) of the E-wave.¹⁷ Chamber stiffness (dP/dV) is linearly related to the spring constant k (g/s^2),^{17,23} while the chamber viscoelasticity/relaxation index c (g/s) characterizes the resistance of the process.^{17,22} E-waves with long concave up deceleration portions ('delayed relaxation pattern') are fit by the overdamped solution and have higher c values, while E-waves that approximate nearly symmetric sine waves are fit by the underdamped solution and have lower c values.¹⁸

Briefly, echocardiographic images are cropped, the mitral E-wave maximum velocity envelopes are identified and fit by the PDF generated solution using the Levenberg-Marquardt algorithm to yield the best-fit PDF parameter x_0 , c , and k , values. The process is achieved using a custom LabVIEW (National Instruments, Austin,

TX) interface.³⁸ In addition to providing parameter values the algorithm also provides a simultaneous measure of goodness of fit. Additional PDF-derived indexes include the stored elastic strain energy available for ventricular suction ($1/2kx_0^2$) at the onset of filling, and the peak atrio-ventricular pressure gradient (kx_0).^{21,24}

As in previous work,^{19,39} interobserver variability in applying the PDF formalism for E-wave analysis was $\leq 8\%$.

Appendix 2

Determination of stiffness and relaxation components of E-wave deceleration time

PDF model predicts that E-wave deceleration time (DT) is a function of both stiffness and relaxation.¹⁸ PDF-based E-wave analysis provides a method for fractionating total DT into its stiffness (DT_s) and relaxation (DT_r) components such that $DT=DT_s+DT_r$. The fractionation method has been previously validated with DT_s and DT_r correlating with simultaneous stiffness (dP/dV) and relaxation (τ) with $r=0.82$ and $r=0.94$ respectively.¹⁹

The duration of the E-wave, AT, and DT are measured as usual from Doppler echo images using a triangle to approximate E-wave shape (Figure 7). The effect of delayed relaxation on an ideal (generated by recoil only) E-wave is to decrease its peak amplitude and lengthen its DT. Accordingly, DT_r is determined by using the same x_0 and k as the original E-wave but setting $c=0$ and thereby providing the PDF generated ideal contour. Subtracting the ideal E-wave duration from actual total duration yields DT_r (See Figure 7). Therefore, E-wave DT is decomposed into its determinants as $DT = DT_s + DT_r$. It is known that DT_s , DT_r are only weakly load and heart rate dependent.¹⁹

References:

1. Cha Y-M, Redfield MM, Shen W-K, and Gersh BJ. Atrial fibrillation and ventricular dysfunction: A vicious electromechanical cycle. *Circulation*. 2004; 109: 2839-2843.
2. Dries D, Exner D, Gersh B, Domanski M, Waclawiw M, and Stevenson L. Atrial fibrillation is associated with an increased risk for mortality and heart failure progression in patients with asymptomatic and symptomatic left ventricular systolic dysfunction: A retrospective analysis of the SOLVD trials. *J. Am. Coll. Cardiol*. 1998; 32: 695-703.
3. Li D, Fareh S, Leung TK, and Nattel S. Promotion of Atrial Fibrillation by Heart Failure in Dogs: Atrial Remodeling of a Different Sort. *Circulation*. 1999; 100: 87-95.
4. Wang TJ, Larson MG, Levy D, Vasan RS, Leip EP, Wolf PA, D'Agostino RB, Murabito JM, Kannel WB, and Benjamin EJ. Temporal relations of atrial fibrillation and congestive heart failure and their joint influence on mortality: The Framingham heart study. *Circulation*. 2003; 107: 2920-2925.
5. Allesie M, Ausma J, and Schotten U. Electrical, contractile and structural remodeling during atrial fibrillation. *Cardiovasc. Res*. 2002; 54: 230-246.
6. Bosch RF, Zeng X, Grammer JB, Popovic K, Mewis C, and Kuehlkamp V. Ionic mechanisms of electrical remodeling in human atrial fibrillation. *Cardiovasc. Res*. 1999; 44: 121-131.
7. Casaclang-Verzosa G, Gersh BJ, and Tsang TSM. Structural and functional remodeling of the left atrium: Clinical and therapeutic implications for atrial fibrillation. *J. Am. Coll. Cardiol*. 2008; 51: 1-11.
8. Everett TH, IV, Li H, Mangrum JM, McRury ID, Mitchell MA, Redick JA, and Haines DE. Electrical, morphological, and ultrastructural remodeling and reverse remodeling in a canine model of chronic atrial fibrillation. *Circulation*. 2000; 102: 1454-1460.

9. Falk RH. Atrial fibrillation. *N. Engl. J. Med.* 2001; 344: 1067-1078.
10. Nattel S. New ideas about atrial fibrillation 50 Years On. *Nature* 2002; 415: 219-226.
11. Kass DA. Assessment of diastolic dysfunction: Invasive modalities. *Cardiol. Clin.* 2000; 18: 571-586.
12. Oh JK, Appleton CP, Hatle LK, Nishimura RA, Seward JB, and Tajik AJ. The non-invasive assessment of left ventricular diastolic function with two-dimensional and Doppler echocardiography. *Journal of the American Society of Echocardiography: official publication of the American Society of Echocardiography.* 1997; 10: 246-270.
13. Zile MR, Baicu CF, and Gaasch WH. Diastolic heart failure--abnormalities in active relaxation and passive stiffness of the left ventricle. *N Engl J Med* 2004; 350: 1953-1959.
14. Zile MR and Brutsaert DL. New concepts in diastolic dysfunction and diastolic heart failure: Part I: diagnosis, prognosis, and measurements of diastolic function. *Circulation.* 2002; 105: 1387-1393.
15. Mossahebi S, Shmuylovich L, Kovács SJ. The challenge of Chamber Stiffness determination in chronic atrial fibrillation vs. normal sinus rhythm: Echocardiographic prediction with simultaneous hemodynamic validation. *J. Afib.* 2013; 6(3): 45-50.
16. Little WC, Ohno M, Kitzman DW, Thomas JD, Cheng CP. Determination of left ventricular chamber stiffness from the time for deceleration of early left ventricular filling. *Circulation.* 1995; 92: 1933-1939.
17. Kovács SJ, Sester R, Hall AF. Left ventricular chamber stiffness from model-based image processing of transmitral Doppler E-waves. *Cor. Art. Dis.* 1997; 8: 179-187.
18. Shmuylovich L, Kovács SJ. E-wave deceleration time may not provide an accurate determination of left ventricular chamber stiffness if left ventricular relaxation/viscoelasticity is unknown. *Am. J. Physiol. Heart Circ. Physiol.* 2007; 292: H2712-H2720.
19. Mossahebi S, Kovács SJ. Kinematic modeling based decomposition of transmitral flow (Doppler E-wave) deceleration time into stiffness and relaxation components. *Cardiovascular Engineering & Technology.* 2014; 5(1): 25-34.
20. Chung CS, Ajo DM, Kovács SJ. Isovolumic pressure-to-early rapid filling decay rate relation: model-based derivation and validation via simultaneous catheterization echocardiography. *J. Appl. Physiol.* 2006; 100: 528-534.
21. Bauman L, Chung CS, Karamanoglu M, Kovács SJ. The peak atrioventricular pressure gradient to transmitral flow relation: kinematic model prediction with in vivo validation. *J. Am. Soc. Echocardiogr.* 2004; 17: 839-844.
22. Kovács SJ, Meisner JS, Yellin EL. Modeling of diastole. *Cardiol. Clin.* 2000; 18: 459-487.
23. Lisauskas JB, Singh J, Bowman AW, Kovács SJ. Chamber properties from transmitral flow: prediction of average and passive left ventricular diastolic stiffness. *J. Appl. Physiol.* 2001; 91: 154-162.
24. Mossahebi S, Shmuylovich L, Kovács SJ. The thermodynamics of diastole: kinematic modeling based derivation of the P-V loop to transmitral flow energy relation, with in-vivo validation. *Am. J. Physiol. Heart Circ. Physiol.* 2011; 300: H514-H521.
25. Gottdiener JS, Bednarz J, Devereux R, Gardin J, Klein A, Manning WJ, Morehead A, Kitzman D, Oh J, Quinones M, Schiller NB, Stein JH, Weissman NJ; American Society of Echocardiography recommendations for use of echocardiography in clinical trials. *J. Am. Soc. Echocardiogr.* 2004; 17: 1086-1119.
26. Nagueh SF, Appleton CP, Gillebert TC, Marino PN, Oh JK, Smiseth OA, Waggoner AD, Flachskampf FA, Pellikka PA, Evangelista A. Recommendations for the evaluation of left ventricular diastolic function by echocardiography. *J. Am. Soc. Echocardiogr.* 2009; 22(2): 107-133.
27. Appleton CP, Firstenberg MS, Garcia MJ, Thomas JD. The echo-Doppler evaluation of left ventricular diastolic function. A current perspective. *Cardiology Clinics.* 2000; 18: 513-546.
28. Feigenbaum H. *Echocardiography.* Baltimore, MD: Williams & Wilkins. 1993; p. 677.
29. Kovács SJ, Barzilai B, Pérez JE. Evaluation of diastolic function with Doppler echocardiography: the PDF formalism. *Am. J. Physiol.* 1987; 87: H178-H187.
30. Kovács SJ, McQueen MD, Peskin CS. Modelling cardiac fluid dynamics and diastolic function. *Philosophical Transactions of the Royal Society (A).* 2001; 359: 1299-1314.
31. Mossahebi S, Kovács SJ. Kinematic modeling-based left ventricular diastatic (passive) chamber stiffness determination with in-vivo validation. *Annals BME.* 2012; 40(5): 987-995.
32. Zhang W, Kovács SJ. The diastatic pressure-volume relationship is not the same as the end-diastolic pressure-volume relationship. *Am. J. Physiol. Heart Circ. Physiol.* 2008; 294(6): H2750-H2760.
33. Zhang W, Shmuylovich L, Kovács SJ. The E-wave delayed relaxation pattern to LV pressure contour relation: model-based prediction with in-vivo validation. *Ultrasound Med. Biol.* 2010; 36: 497-511.
34. Garcia MJ, Firstenberg MS, Greenberg NL, Smedira N, Rodriguez L, Prior D, and Thomas JD. Estimation of left ventricular operating stiffness from Doppler early filling deceleration time in humans. *Am. J. Physiol.* 2001; 280: H554-561.
35. Ohno M, Cheng C, and Little W. Mechanism of altered patterns of left ventricular filling during the development of congestive heart failure. *Circulation.* 1994; 89: 2241-2250.
36. Zhang W, Chung CS, Shmuylovich L, and Kovács SJ. Viewpoint: Is Left Ventricular Volume During Diastasis the Real Equilibrium Volume and, What Is Its Relationship to Diastolic Suction? *J. Appl. Physiol.* 2008; 105: 1012-1014.
37. Chung CS, and Kovács SJ. Consequences of increasing heart rate on deceleration time, the velocity-time integral, and E/A. *Am. J. Cardiol.* 2006; 97: 130-136.
38. Hall AF, Kovács SJ. Automated method for characterization of diastolic transmitral Doppler velocity contours: early rapid filling. *Ultrasound Med. Biol.* 1994; 20: 107-116.
39. Boskovski M, Shmuylovich L, Kovács SJ. Transmitral flow velocity-contour variation after premature ventricular contractions: A novel test of the load-independent index of diastolic filling. *Ultrasound Med. Biol.* 2008; 34(12): 1901-1908.